Bioorganic & Medicinal Chemistry Letters 24 (2014) 337–343

Contents lists available at ScienceDirect

Bioorganic & Medicinal Chemistry Letters

journal homepage: www.elsevier.com/locate/bmcl

Discovery of potent and efficacious cyanoguanidine-containing nicotinamide phosphoribosyltransferase (Nampt) inhibitors

Xiaozhang Zheng [a,*], Timm Baumeister [a], Alexandre J. Buckmelter [a], Maureen Caligiuri [a], Karl H. Clodfelter [a], Bingsong Han [a], Yen-Ching Ho [a], Nikolai Kley [a], Jian Lin [a], Dominic J. Reynolds [a], Geeta Sharma [a], Chase C. Smith [a], Zhongguo Wang [a], Peter S. Dragovich [b], Angela Oh [b], Weiru Wang [b], Mark Zak [b], Yunli Wang [c], Po-wai Yuen [c], Kenneth W. Bair [a]

[a] Forma Therapeutics, Inc., 500 Arsenal Street, Watertown, MA 02472, USA
[b] Genentech, Inc., 1 DNA Way, South San Francisco, CA 94080, USA
[c] Pharmaron Beijing, Co. Ltd, 6 Tai He Road, BDA, Beijing 100176, PR China

ARTICLE INFO

Article history:
Received 6 September 2013
Revised 1 November 2013
Accepted 5 November 2013
Available online 14 November 2013

Keywords:
Nicotinamide phosphoribosyltransferase
Nampt
cyanoguanidine
X-ray crystal structure

ABSTRACT

A co-crystal structure of amide-containing compound (**4**) in complex with the nicotinamide phosphoribosyltransferase (Nampt) protein and molecular modeling were utilized to design and discover a potent novel cyanoguanidine-containing inhibitor bearing a sulfone moiety (**5**, Nampt Biochemical IC_{50} = 2.5 nM, A2780 cell proliferation IC_{50} = 9.7 nM). Further SAR exploration identified several additional cyanoguanidine-containing compounds with high potency and good microsomal stability. Among these, compound **15** was selected for in vivo profiling and demonstrated good oral exposure in mice. It also exhibited excellent in vivo antitumor efficacy when dosed orally in an A2780 ovarian tumor xenograft model. The co-crystal structure of this compound in complex with the NAMPT protein was also determined.

Nicotinamide adenine dinucleotide (NAD) is an abundant and essential biomolecule used as a co-factor and/or substrate for many biological processes.[1] Mammals have multiple biosynthetic pathways to produce NAD; a de novo pathway using tryptophan and three pathways using exogenous biomolecules as the precursors—nicotinamide (NAM), nicotinic acid (NA), and nicotinamide ribose (NR).[2] NAM can be converted to NAD via a two-step pathway that uses nicotinamide phosphoribosyltransferase (Nampt) as the rate limiting enzyme (Fig. 1a). In an ATP hydrolysis coupled reaction, Nampt catalyzes the formation of NAD through the condensation of NAM with 5-phosphoribosyl-1-pyrophosphate (PRPP) to form nicotinamide mononucleotide (NMN), the immediate precursor to NAD (Fig. 1b).[3] NAD can be consumed in a manner that releases nicotinamide (NAM) by enzymes which catalyze mono- and poly-(ADP)-ribosylations, NAD dependent-protein deacetylations (Sirutins), and cyclic-ADP-ribose production. The primary mechanism of maintaining intracellular NAD levels is its synthesis from released NAM via the Nampt-dependent salvage pathway.[4] In cancers, elevated poly-ADP-ribose polymerase (PARP) activity has been well documented, which leads to an elevated rate of cellular NAD consumption. As a co-factor, NAD and its reduced form NADH are used in multiple biological redox reactions such as mitochondrial oxidative phosphorylation, glycolysis, and the citric acid cycle. These processes are used to produce ATP and assorted essential biosynthetic precursors upon whose levels cancer cells are exquisitely dependent. Additionally, NAD and NADH have essential functions in maintaining the reductive environment that protects cells from reactive oxygen species which are elevated in cancers.[5] Cancer cells that consume more NAD and are more dependent upon NAD driven processes should be extremely sensitive to inhibition of the NAD salvage pathway. Therefore, Nampt is an inviting target for potential development of novel cancer therapies.

Several classes of Nampt inhibitors have been reported in the scientific literature[6,7] and the most advanced compounds GMX-1778[8] (**1**), its prodrug GMX-1777[9] (not shown), and APO-866[10] (**2**) progressed to clinical trials during the past decade (Fig. 2). We recently reported the structure-based identification of urea- and amide-containing Nampt inhibitors, exemplified by compounds **3** and **4** (Fig. 2).[11,12] In the current work, we describe the continuation of our Nampt-related research leading to the discovery of novel and highly potent cyanoguanidine-containing Nampt inhibitors.

Our previous exploration of urea- and amide-containing Nampt inhibitors indicated that changes within the linker region of the compounds were tolerated as long as the positioning of the left hand side (LHS) aromatic ring and the right hand side (RHS) moiety remained unaffected (Fig. 3). In particular, crystallographic water

* Corresponding author.
E-mail address: xzheng@formatherapeutics.com (X. Zheng).

0960-894X/$ - see front matter © 2013 Elsevier Ltd. All rights reserved.
http://dx.doi.org/10.1016/j.bmcl.2013.11.006

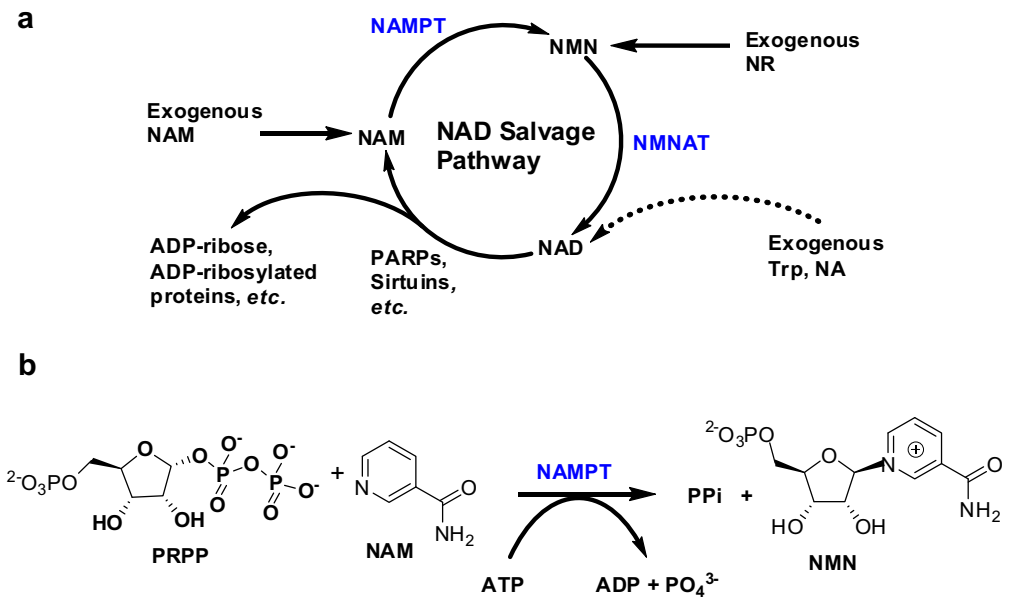

Figure 1. (a) Schematic representation of NAD biosynthetic pathways found in mammalian cells. Nampt, the rate limiting step in the biosynthesis of NAD from NAM, catalyzes the conversion of NAM to NMN. NMN is further converted to NAD by the enzyme nicotinamide mononucleotide adenylyltransferase (NMNAT). NAD can also be produced through alternative pathways using Trp (tryptophan), NA (nicotinic acid), and NR (nicotinamide ribose) as the precursors. (b) The phosphoribosyltransferase reaction catalyzed by Nampt.

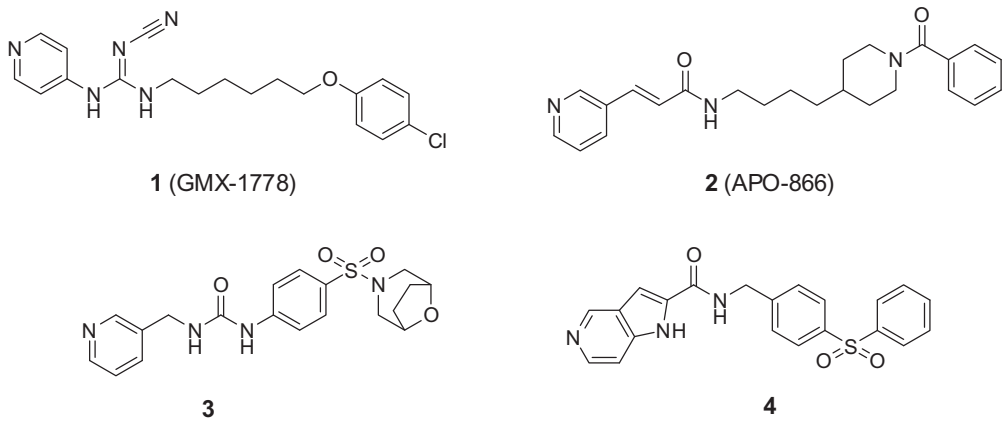

Figure 2. Examples of Nampt inhibitors.

molecules in the linker region shifted to accommodate variation in the linker hydrogen bonding network between Nampt residues Ser275 and Asp219.[11,12] To further examine the effects of different linker groups, we used molecular modeling to explore whether the cyanoguanidine linker in compound **1** could replace the amide moiety present in compound **4**, for which a co-crystal structure in complex with NAMPT was obtained (Fig. 3). The docked pose of the resulting hybrid molecule **5** overlapped well with both the pyridine and cyanoguanidine portion of docked **1** as well as with the RHS of compound **4** (Fig. 4). Compound **5** was therefore synthesized, and it demonstrated very good biochemical and cellular *anti*-Nampt potency (Table 1).[13] The molecule thus provided an excellent starting point for further inhibitor optimization.

As shown in Table 1, a compound containing a sulfonamide RHS moiety was also a potent Nampt inhibitor in biochemical and cell-based assays. Interestingly, moving the pyridine nitrogen atom from the 4-position to 3-position (compounds **7** and **8**) resulted in equal biochemical potency but also produced a several-fold loss of cellular activity (compare to **5** and **6**). The reduced cell potencies of **7** and **8** relative to **5** and **6** may be due to improper positioning of the LHS pyridine atom which prevents facile formation of the corresponding inhibitor-PRPP ribose adducts in the Nampt active site.[15] The sulfone containing compounds (**5** and **7**) displayed better mouse liver microsomal stability than the sulfonamide-containing inhibitors (**6** and **8**), and this trend was also observed with other Nampt inhibitors we previously studied.[11,12]

With this information, our research then focused on 4-pyridine-cyanoguanidine sulfones by exploring various substituents on the RHS of the molecules. Our previous work with related urea- and amide-containing compounds indicated that alterations to the biarylsulfone portion of the inhibitor could greatly improve the potency and biopharmaceutical properties.[11,12] Similar modifications were expected to be tolerated in the cyanoguanidine-containing Nampt inhibitor series since the biarylsulfone terminus was anticipated to be highly solvent-exposed. As shown in Table 2, inserting a methylene group between the sulfone and phenyl ring led to compound **9** which maintained good biochemical activity

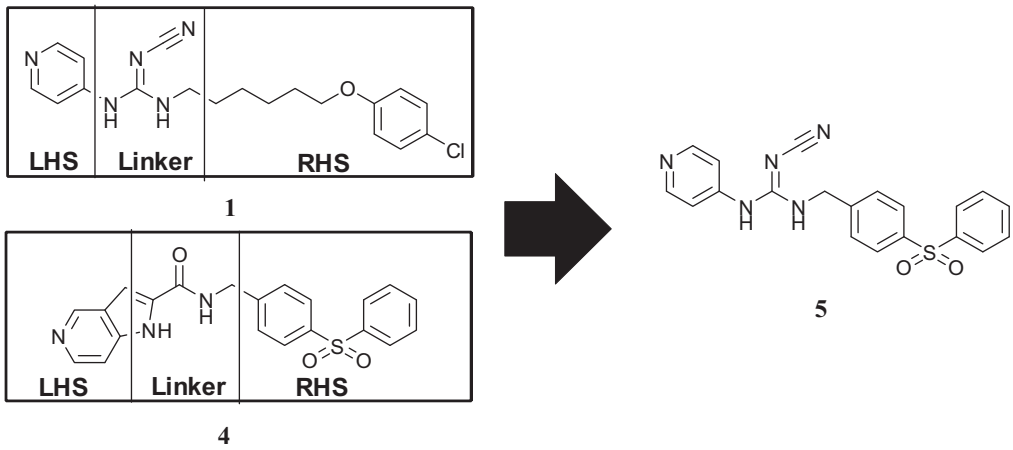

Figure 3. Discovery of novel cyanoguanidine-containing Nampt inhibitors.

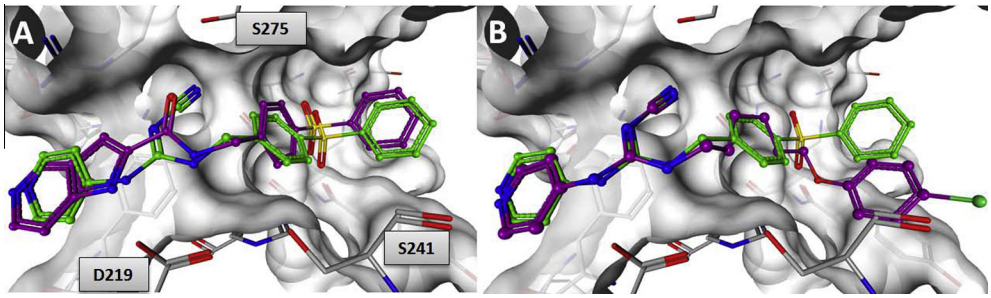

Figure 4. Overlay of compound **5** (green carbons) with: (A) compound **4** from PDB code 4LWW and (B) compound **1** (each in magenta) in complex with Nampt (grey). The structure of compounds **5** and **1** represent minimum energy conformations obtained from docking with GlideXP.[14]

Table 1
Initial SAR of cyanoguanidine-containing Nampt inhibitors

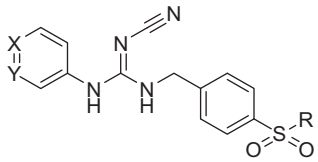

Entry	X	Y	R	Nampt IC_{50}[a,c] (nM)	A2780 IC_{50}[b,c] (nM)	MLM % remaining[d]	HLM % remaining[e]
4[f]				29	18	54	75
5	N	CH		2.5	9.7	57	96
6	N	CH	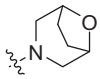	2.4	50	12	60
7	CH	N		2.2	30	14	83
8	CH	N	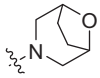	4.4	175	5.5	52

[a] Nampt biochemical inhibition.
[b] A2780 cell proliferation inhibition. This inhibition can be reversed by addition of 0.33 mM of NMN.
[c] Unless otherwise noted, all biochemical and cell-based assay results are reported as the arithmetic mean of at least 2 separate runs ($n = 2$).
[d] Mouse liver microsomal stability—% remaining at 30 min.
[e] Human liver microsomal stability—% remaining at 30 min.
[f] For structure see Figure 2.

Table 2
RHS SAR of cyanoguanidine-containing Nampt inhibitors

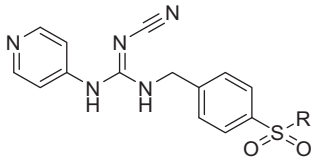

Entry	R	Nampt IC_{50}[a,c] (nM)	A2780 IC_{50}[b,c] (nM)	MLM % remaining[d]	HLM % remaining[e]	Solubility[f] (μM)
9	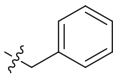	7.5	264	27	27	30
10		5.4	14.8	0.3	56	ALQ[g]
11		2.0	>2000	49	89	NA[h]
12	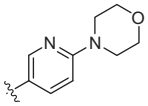	1.7	3.7	67	85	67
13	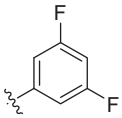	0.6	1.8	71	83	1.3
14	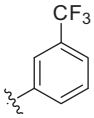	2.4	2.9	74	62	28
15	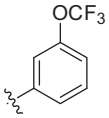	4.4	2.2	55	45	16
16	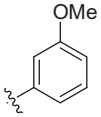	1.9	3.4	58	55	51
17	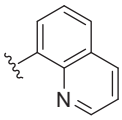	3.6	14	11	10	18

[a] Nampt biochemical inhibition.
[b] A2780 cell proliferation inhibition. This inhibition can be reversed by addition of 0.33 mM of NMN.
[c] Unless otherwise noted, all biochemical and cell-based assay results are reported as the arithmetic mean of at least 2 separate runs ($n = 2$).
[d] Mouse liver microsomal stability—% remaining at 30 min.
[e] Human liver microsomal stability—% remaining at 30 min.
[f] Aqueous solubility.
[g] Above Limit of Quantification (>100 μM).
[h] Not Available.

but displayed greatly reduced cellular potency. The conversion of the terminal phenyl ring of compound **5** to a cyclohexyl moiety (compound **10**), did not impact potency but resulted in a significant loss of mouse liver microsome stability. Incorporating a nitrogen atom into the terminal ring (compound **11**) maintained biochemical potency but led to a dramatic loss of cellular activity. However, introducing a morpholino group attached to a terminal pyridine ring (compound **12**) greatly improved the cellular potencies. Modification of the terminal phenyl ring by introducing substituents such as 3,5-di-F, 3-CF_3, 3-OCF_3, and 3-OMe afforded very potent Nampt inhibitors in both biochemical and cell-based assessments (**13**–**16**). A fused bicyclic aryl terminal system (**17**) maintained good biological activities but also exhibited impaired microsomal stabilities. In summary, RHS SAR exploration led to the discovery of several potent Nampt inhibitors with good microsomal stability as well as acceptable aqueous solubility.

Among the potent and stable compounds, **15** was selected to progress to in vivo mouse PK and xenograft efficacy studies. As shown in Table 3, compound **15** exhibited good exposures in mice following oral administration using a solution formulation. As depicted in Figure 5, compound **15** also displayed robust efficacy in an A2780 human ovarian carcinoma xenograft model with relatively minor changes in body weights. Encouragingly, oral administration of the compound for 5 days (75 mg/kg BID; maximum tolerated dose) produced rapid tumor regression. The *anti*-tumor effects exhibited by compound **15** were durable, with the mean tumor volume of the treated group failing to return to baseline levels by the end of the study (day 13). The described xenograft

Table 3
Compound **15** in vivo mouse PK parameters after oral administration (75 mg/kg)

PK parameters	Mean (n = 3) ± SD
C_{max} (μM)	47.9 ± 17.5
T_{max} (h)	2.00
AUC_{inf} (μM h)	286.8 ± 194.1
$t_{1/2}$(h)	2.16

results confirmed that a cyanoguanidine-containing Nampt inhibitor with appropriate biological and PK properties can function as a potent in vivo *anti*-cancer agent.

To enable further optimization of the described cyanoguanidine-containing Nampt inhibitors, we obtained a co-crystal structure of compound **15** in complex with the protein (Fig. 6B). The right hand side of **15** closely overlapped with the co-crystal of **4** and with structures of our other previously disclosed urea-, thiourea-, and amide-containing inhibitors.[11,12] The cyano nitrogen of **15** was located at a position close to that occupied by the sulfur atom of our related thiourea inhibitor (PDB code 4JRS)[11a] and formed a direct hydrogen bond with Ser275 while replacing the and displaced a crystallographic water that mediated a similar interaction in the structure of **4**. The two NH groups of **15** formed direct hydrogen bonds with Asp219 in contrast to a related thiourea inhibitor whose interactions with Asp219 were mediated by a crystallographic water molecule.[11a] For both **4** and **15**, the sulfone oxygens formed water mediated hydrogen bonds with the backbone carbonyls of Val350 and Tyr188. The trifluoromethoxy group of **15** was positioned in a pocket surrounded by the residues of His191, Val242, Ser241, Tyr240, and Tyr188. This orientation left considerable space for ligand expansion in the vicinity of the terminal phenyl ring and explained the wide tolerance of various terminal sulfones noted in the SAR.

The inhibitors described in this work were prepared by the general synthetic method depicted in Scheme 1. Commercially available dimethyl cyanocarbonimidodithioate (**18**) was reacted with 3 or 4-aminopyridines (**19**) under basic conditions to afford cyanocarbonimidothioate intermediates (**20**) which were subsequently condensed with a variety of benzylamines (**21**) to provide the desired products **5**–**17**.

The synthesis of benzylamine **21a** is shown in Scheme 2. Sulfonyl chloride (**22**) was coupled with bridged morpholine (**23**) to provide the corresponding sulfonamide (**24**). This intermediate was then reduced to the benzylamine (**21a**) by hydrogenation.

The preparation of benzylamine **21b** is depicted in Scheme 3. Sulfinate (**25**)[16] was coupled with benzyl bromide (**26**) to provide the corresponding sulfone intermediate (**27**). Removal of the acetyl group from **27** then led to the benzyl amine **21b**.

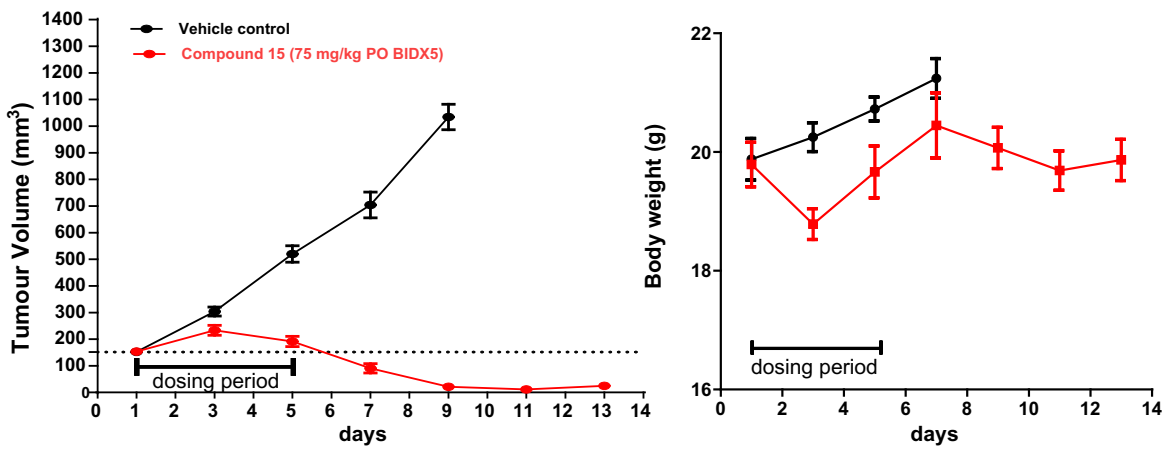

Figure 5. Left panel: efficacy of compound **15** (dosed 75 mg/kg BID) in A2780 mouse xenograft model. Right panel: body weight loss as a result of compound **15** administration in xenograft experiment. Eight (8) mice were employed per group. Vehicle = 60% PEG400/10% EtOH/30% D5W. Data reflect mean values (± standard deviation).

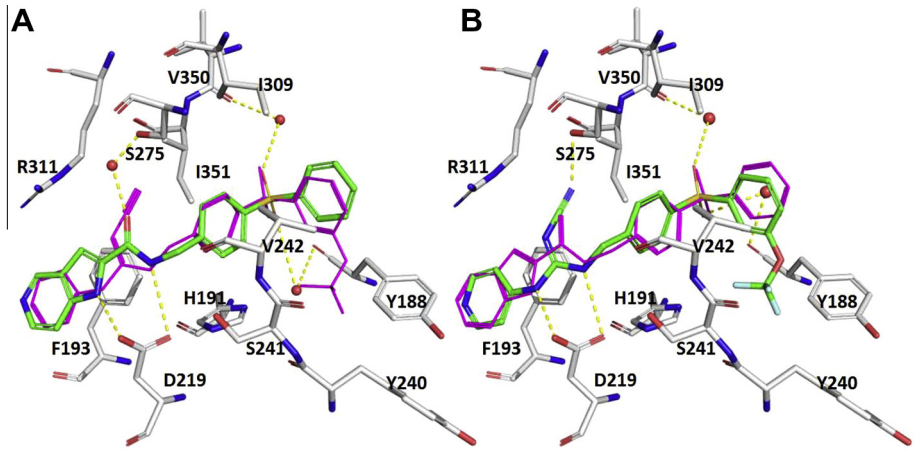

Figure 6. (A) Co-crystal structure of **4** (green carbons) in complex with NAMPT (PDB code 4LWW, resolution 1.64 Å). (B) Co-crystal structure of **15** (green carbons) in complex with Nampt (PDB code 4LTS, resolution 1.70 Å). Important crystallographic waters present in each structure are shown as red spheres, and possible hydrogen bonds are depicted as dashed yellow lines. For comparison, each picture shows the overlay of the ligand of the other structure in magenta.

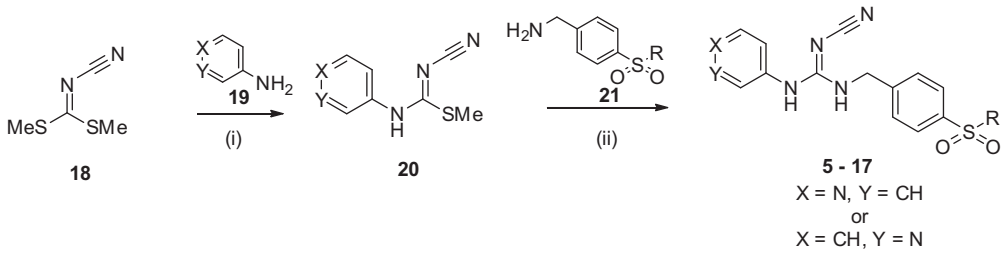

Scheme 1. Synthesis of cyanoguanidine-containing compounds. Reagents and conditions: (i) NaH, DMAP, DMF, 0 to 25 °C, 18 h, 39–84%; (ii) Et_3N, DMAP, pyridine, 60 °C, 12 h, 36–73%.

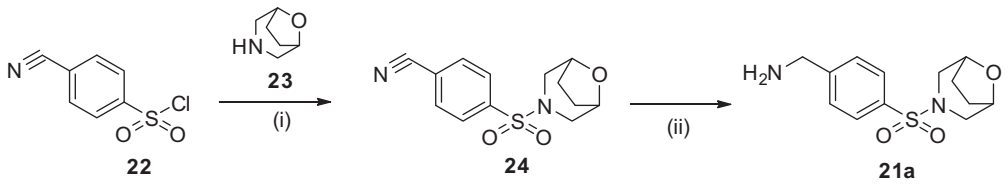

Scheme 2. Synthesis of compound **21a**. Reagents and conditions: (i) $(i\text{-Pr})_2NEt$, CH_2Cl_2, 0 to 25 °C, 2 h, 78%; (ii) Raney Ni, H_2, 45 psi, MeOH, 100 °C, 16 h, 58%.

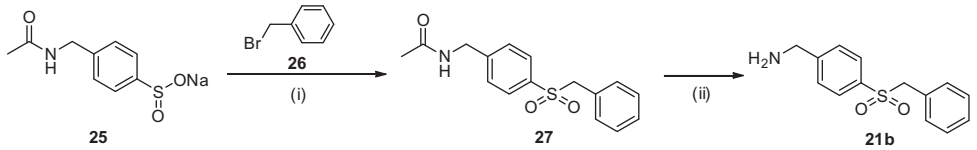

Scheme 3. Synthesis of compound **21b**. Reagents and conditions: (i) $(n\text{-Bu})_4N^+I^-$, H_2O, 70 °C, 2 h, 54%; (ii) 12 M HCl-*i*-PrOH, 100 °C, 16 h, 80%.

The synthesis of compound **21c** is shown in Scheme 4. Treatment of 4-fluorobenzonitrile (**28**) with cyclohexanethiol (**29**) gave the thioether intermediate (**30**). Oxidation of **30** with mCPBA provided the corresponding sulfone (**31**) which was then reduced to compound **21c**.

The preparation of benzylamines (**21d**–**21k**) is described in Scheme 5. Sulfinate (**28**) underwent Chan–Lam oxidative coupling with aryl boronic acids (**32**) to provide the corresponding biaryl sulfone intermediates (**33**). Removal of the acetyl group from **33** led to the benzyl amines **21d**–**21k**.

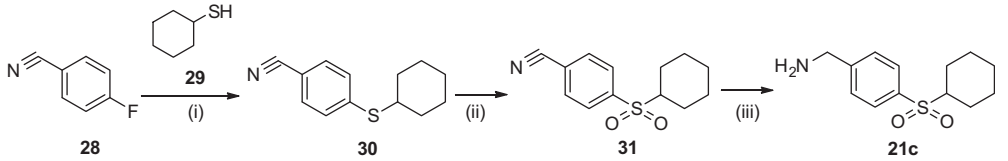

Scheme 4. Synthesis of compound **21c**. Reagents and conditions: (i) K_2CO_3, DMF, 120 °C, 20 h, 84%; (ii) mCPBA, CH_2Cl_2, 25 °C, 4 h, 70%; (iii) 10% Pd/C, H_2, 45 psi, MeOH, 25 °C, 1 h, 43%.

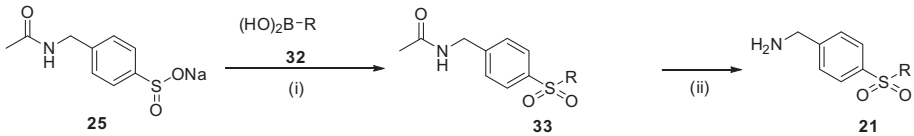

Entry	R
21d	phenyl
21e	3-pyridyl
21f	3-(6-morpholino)-3-pyridiyl
21g	3,5-di-F-phrnyl
21h	3-CF_3-phenyl
21i	3-OCF_3-phenyl
21j	3-OMe-phenyl
21k	8-quinolinyl

Scheme 5. Synthesis of compounds **21d**–**21k**. Reagents and conditions: (i) $Cu(OCOCH_3)_2$, K_2CO_3, DMSO, 25 °C, 16 h, 15–45%; (ii) 12 M HCl-*i*-PrOH, 100 °C, 16 h, 80–100%.

As described above, we identified novel and potent Nampt inhibitors which contain the cyanoguanidine moiety. Several of these compounds exhibit nanomolar antiproliferative activity against human tumor lines in in vitro cell culture experiments, and a representative example (compound **15**) demonstrated good mouse PK properties and was efficacious in an A2780 mouse xenograft model. A co-crystal structure of compound **15** obtained in complex with Nampt suggested additional possibilities for future inhibitor modification.

Acknowledgments

We acknowledge Forma's high speed synthesis group for their synthetic contributions and the ADME group for generating the microsomal and solubility data, Shohini Ganguly and Rashida Garcia-Dancey for helping to generate the cellular data, Lakshmanan Manikandan, Saradhi Vijay, and Danilal C. Sharma for generating the in vivo PK and efficacy data, Agilent Technologies (Woburn, MA) for generating the Rapidfire LCMS data, and Professor Yigong Shi's group (Tsinghua University, Beijing, China) for providing a Nampt DNA construct and Nampt protein.

Supplementary data

Supplementary data associated with this article can be found, in the online version, at http://dx.doi.org/10.1016/j.bmcl.2013.11.006.

References and notes

1. Houtkooper, R. H.; Cantó, C.; Wanders, R. J.; Auwerx, J. *Endocr. Rev.* **2010**, *31*, 194.
2. Belenky, P.; Bogan, K. L.; Brenner, C. *Trends Biochem. Sci.* **2007**, *32*, 12.
3. (a) Revollo, J. R.; Grimm, A. A.; Imai, S. *J. Biol. Chem.* **2004**, *279*, 50754; (b) Galli, M.; Van Gool, F.; Rongvaux, A.; Andris, F.; Leo, O. *Cancer Res.* **2010**, *70*, 8; (c) Garten, A.; Petzold, S.; Korner, A.; Imai, S.-I.; Kiess, W. *Trends Endocrinol. Metab.* **2009**, *20*, 130.
4. (a) Zaremba, T.; Ketzer, P.; Cole, M.; Coulthard, S.; Plummer, E. R.; Curtin, N. J.; Brit, J. *Cancer* **2009**, *101*, 256; (b) Khan, J. A.; Forouhar, F.; Tao, X.; Tong, L. *Exp. Opin. Ther. Targets* **2007**, *11*, 695.
5. (a) Koppenol, W. H.; Bounds, P. L.; Dang, C. V. *Nat. Rev. Cancer* **2011**, *11*, 325; (b) Ward, P. S.; Thompson, C. B. *Cancer Cell* **2012**, *21*, 297; (c) Cerna, D.; Li, H.; Flaherty, S.; Takebe, N.; Coleman, C.; Yoo, S. S. *J. Biol. Chem.* **2012**, *287*, 22408; (d) Vander Heiden, M. G.; Cantley, L. C.; Thompson, C. B. *Science* **2009**, *5930*, 1029.
6. He, J.; Tu, C.; Li, M.; Wang, S.; Guan, X.; Lin, J.; Li, Z. *Curr. Pharm. Des.* **2012**, *18*, 6123.
7. Burgos, E. S. *Curr. Med. Chem.* **2011**, *18*, 1947.
8. (a) Watson, M.; Roulston, A.; Bélec, L.; Billot, X.; Marcellus, R.; Bédard, D.; Bernier, C.; Branchaud, S.; Chan, H.; Dairi, K.; Gilbert, K.; Goulet, D.; Gratton, M.-O.; Isakau, H.; Jang, A.; Khadir, A.; Koch, E.; Lavoie, M.; Lawless, M.; Nguyen, M.; Paquette, D.; Turcotte, E.; Berger, A.; Mitchell, M.; Shore, G. C.; Beauparlant, P. *Mol. Cell. Biol.* **2009**, *29*, 5872; (b) Ravaud, A.; Cerny, T.; Terret, C.; Wanders, J.; Bui, B. N.; Hess, D.; Droz, J.-P.; Fumoleau, P.; Twelves, C. *Eur. J. Cancer* **2005**, *41*, 702; (c) Hovstadius, P.; Larsson, R.; Jonsson, E.; Skov, T.; Kissmeyer, A.-M.; Krasilnikoff, K.; Bergh, J.; Karlsson, M. O.; Lönnebo, A.; Ahlgren, J. *Clin. Cancer Res.* **2002**, *8*, 2843. Compound **1** is also known in the literature as CHS828.
9. Beauparlant, P.; Bédard, D.; Bernier, C.; Chan, H.; Gilbert, K.; Goulet, D.; Gratton, M.-O.; Lavoie, M.; Roulston, A.; Turcotte, E.; Watson, M. *Anti-Cancer Drugs* **2009**, *20*, 346.
10. (a) Olesen, U. H.; Thougaard, A. V.; Jensen, P. B.; Sehested, M. *Mol. Cancer Ther.* **2010**, *9*, 1609; (b) Holen, K.; Saltz, L. B.; Hollywood, E.; Burk, K.; Hanauske, A.-R. *Invest. New Drugs* **2008**, *26*, 45. Compound **2** is also known in the literature as FK866.
11. (a) Zheng, X.; Bauer, P.; Baumeister, T.; Buckmelter, A. J.; Caligiuri, M.; Clodfelter, K. H.; Han, B.; Ho, Y.-C.; Kley, N.; Lin, J.; Reynolds, D. J.; Sharma, G.; Smith, C. C.; Wang, Z.; Dragovich, P. S.; Oh, A.; Wang, W.; Zak, M.; Gunzner-Toste, J.; Zhao, G.; Yuen, P.-w.; Bair, K. W. *J. Med. Chem.* **2013**, *56*, 4921; (b) Gunzner-Toste, J.; Zhao, G.; Bauer, P.; Baumeister, T.; Buckmelter, A. J.; Caligiuri, M.; Clodfelter, K. H.; Fu, B.; Han, B.; Ho, Y.-C.; Kley, N.; Liang, X.; Liederer, B. M.; Lin, J.; Mukadam, S.; O'Brien, T.; Oh, A.; Reynolds, D. J.; Sharma, G.; Skelton, N.; Smith, C. C.; Sodhi, J.; Wang, W.; Wang, Z.; Xiao, Y.; Yuen, P.-w.; Zak, M.; Zhang, L.; Zheng, X.; Bair, K. W.; Dragovich, P. S. *Bioorg. Med. Chem. Lett.* **2013**, *23*, 3531.
12. Zheng, X.; Bauer, P.; Baumeister, T.; Buckmelter, A. J.; Caligiuri, M.; Clodfelter, K. H.; Han, B.; Ho, Y.-C.; Kley, N.; Lin, J.; Reynolds, D. J.; Sharma, G.; Smith, C. C.; Wang, Z.; Dragovich, P. S.; Gunzner-Toste, J.; Liederer, B. M.; Ly, J.; O'Brien, T.; Oh, A.; Wang, L.; Wang, W.; Xiao, Y.; Zak, M.; Zhao, G.; Yuen, P.-w.; Bair, K. W. *J. Med. Chem.* **2013**, *56*, 6413.
13. The antiproliferative effects exhibited in cell culture by **5** were completely reversed when the compound was tested in the presence of 0.33 mM NMN (the product of the Nampt-catalyzed condensation of nicotinamide and PRPP cf., Fig. 1). This result strongly suggests that the observed cell-based effects result from Nampt inhibition. Related NMN experiments were conducted in cell-based assessments with all inhibitors reported in this work and all displayed similar reversals of their antiproliferative effects.
14. Friesner, R. A.; Banks, J. L.; Murphy, R. B.; Halgren, T. A.; Klicic, J. J.; Mainz, D. T.; Repasky, M. P.; Knoll, E. H.; Shaw, D. E.; Shelley, M.; Perry, J. K.; Francis, P.; Shenkin, P. S. *J. Med. Chem.* **2004**, *47*, 1739.
15. We currently believe that many cell-potent NAMPT inhibitors form PRPP-derived phosphoribosylated adducts in the protein's active site which block the function of the enzyme. This belief is consistent with the repeated observation of these adducts by mass spectrometry in biochemical experiments (Refs. 11,12). Once formed, the PRPP-adducts may accumulate intracellularly and thereby enhance cell culture antiproliferation effects (see Ref. 8 for additional information and discussion). However, there are many other factors that also likely influence NAMPT inhibitor cell potency including: biochemical potency, the ability of a given inhibitor and/or its corresponding PRPP-derived ribose adduct to effectively compete with the NAM substrate, cell membrane permeability, and/or protein binding.
16. Bair, K.W. Baumeister, T. Buckmelter, A.J. Clodfelter, K.H. Dragovich, P.S. Gosselin, F. Han, B. Lin, J. Reynolds, D.J. Roth, B. Smith, C.C. Wang, Z. Yuen, P.-w. Zheng, X. WO 2012/031197.